INVERSE AND FORWARD KINEMATICS AND DYNAMICS OF A TWO LINK ROBOT ARM

DARINA HRONCOVA[1], PATRIK SARGA[1], PETER JAN SINCAK[1], TOMAS MERVA[1], LEO BRADA[1]

[1]Technical University of Kosice, Faculty of Mechanical Engineering, Kosice, Slovak Republic

DOI: 10.17973/MMSJ.2023_12_2023067

patrik.sarga@tuke.sk

This paper deals with the kinematic and dynamic analysis of a two-element robot model. We have solved the problem using inverse kinematics. The result is the plotted trajectory of the robot's end point along defined points of the robot's workspace. The angular quantities computed are the rotation angle, angular velocity and angular acceleration in each kinematic pair. Furthermore, an inverse dynamics problem is solved. The moments in the kinematic pairs are computed. Subsequently, using the direct dynamics problem, the correctness of the obtained solution is confirmed. The programs designed for the simulation of dynamical systems - Matlab/Simulink and SimMechanics - were used in the solution. The results are presented in the form of graphs and tables.

KEYWORDS

Robot, trajectory, computer simulation, kinematics, dynamics, forward, inverse, Matlab, Simulink

1 INTRODUCTION

Nowadays, we are experiencing a massive deployment of robots in manufacturing processes. Industrial robots are composed of bodies and form different kinds of kinematic chains. In most cases, the mechanisms of robots and manipulators are open or mixed kinematic chains. The two bodies of a robot kinematic chain are connected to each other such that the motion of one relative to the other is constrained, forming a kinematic pair. They are connected to each other by a joint. In the case of robots, we most often encounter translational or rotational kinematic pairs. The authors [Smrcek 2003, Vagas 2011, Virgala 2012, Bozek 2014, Carbone 2016, Mikova 2016, Papacz 2018] deal with the kinematics of robot mechanisms and similar applications in their works.

Various analytical kinematic methods, geometric methods and experimental methods are used in solving kinematics. Using them, we obtain information about the kinematic quantities of the system at the desired moment of the robot mechanism operation. These methods are then complemented by computer simulations of the many available programs, which by their illustrative nature give more detailed and illustrative information about the behavior of the robot mechanism in the manufacturing process. The problem of computer simulation of robots is discussed in the works of the authors [Kelemen 2014 and 2021, Semjon 2016 and 2020, Tedeschi 2015 and 2017, Bozek 2021, Trojanova 2021].

In this paper, kinematic and dynamic analysis of a model of a two-link robotic arm on a fixed base is performed. The two-link manipulator arm has two members acting in rotational motion. It is attached by a rotational linkage on the lower fixed part. The solution of the problem was implemented in Matlab/Simulink. The result of the solution is an analysis of the motion of the end point of the manipulator arm. The waveforms of angular quantities and driving moments in each kinematic pair were obtained. The trajectory of the end point as a function of time and other kinematic dependencies were determined.

The paper is a demonstration of the use of computer programs in the kinematic and dynamic analysis of multi-link robotic systems. The above-mentioned topic is also discussed by the authors [Frankovsky 2013, Delyova 2014, Mikova 2014, Virgala 2014, Serrano 2015, Zidek 2018, Dyadyura 2021, Kelemenova 2021, Hroncova 2022a,b, Lestach 2022].

2 ANALYTICAL METHODS

The use of analytical methods, which include methods of analytic geometry, tensor and matrix calculus, complex variables, trigonometric, and vector methods, have been discussed in the works of the authors [Holubek 2014, Garcia 2015, Saga 2018, Ruzarovsky 2019, Tlach 2019, Virgala 2020 and 2022, Sincak 2021, Vagas 2022 and 2023, Zivcak 2023].

Nowadays, with the development of computer technology, experimental methods linked with computer systems are used. We can measure the motion parameters during the rewinding of mechanisms, which increases the accuracy of measurements which is the subject of, for example, the works [Hargas 2015, Pirnik 2016, Simonova 2017, Kurylo 2018, Saga 2018 and 2020, Sapietova 2018, Volak 2019, Nikitin 2020 and 2022, Peterka 2020, Pivarciova 2022, Mikova 2022].

Matrix methods, with their matrix notation, which is compact and illustrative, are suitable for use in a computer environment. They are the most used today. They are suitable for numerical methods used on a computer. Kinematic analysis is discussed in the works of [Hroncova 2019, Hunady 2019]. For kinematic and dynamic analysis of robot structures, simulation programs such as Matlab/Simulink are often used.

The following sections of the paper describe the construction of a computer model and then the determination of the trajectory of the robot's end member during its motion.

The inverse kinematics problem was solved first, followed by the direct kinematics problem. In the next section, the inverse problem of dynamics was solved. The solution of the problem is shown on a simple model of a two-link robot, which was executed in Matlab. The dynamics analysis also made use of the Matlab extension Simulink with its SimMechanics library, which was used to solve the inverse dynamics problem. Using it, we determined the waveform of moments in kinematic pairs.

3 MODEL OF MANIPULATOR WITH TWO-LINK ARM

The theory of simple open kinematic chains has direct application in the kinematic analysis of various manipulators and robots, which are often made up of these chains. They can be found as part of multi-link robots with a fixed base (Fig. 1a) or as a superstructure on the chassis of a mobile manipulator (Fig. 1b).

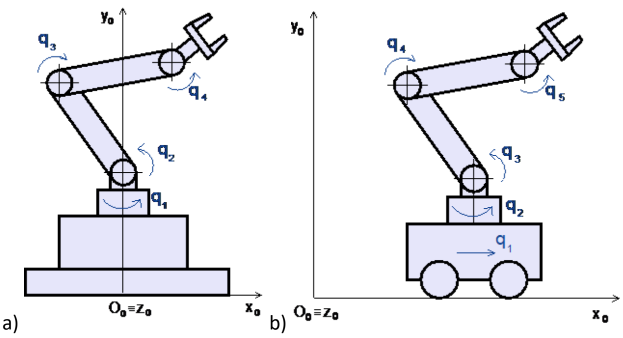

Figure 1. Two-link robotic arm a) on a fixed base, b) on a mobile chassis

The mechanical system of the two-link manipulator in Fig. 2 is an open kinematic chain. The example model of the two-link robotic arm in Fig. 2 was created in MSC Adams View. The end point motion trajectory for the two-link arm is plotted in Fig. 2a) on a fixed base and in Fig. 2b) on a mobile chassis.

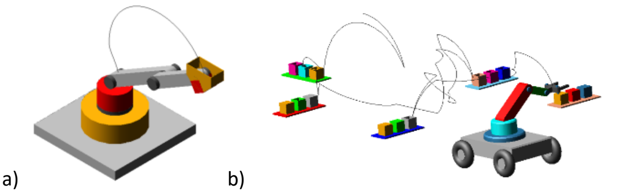

Figure 2. Two-link robotic arm with trajectory of end point in MSC Adams software a) on a fixed arm, b) on a mobile arm

The manipulator model in Fig. 3a) shows the possibilities of moving the end point during the robot's working operation. In Fig. 3b) the manipulator workspace is drawn.

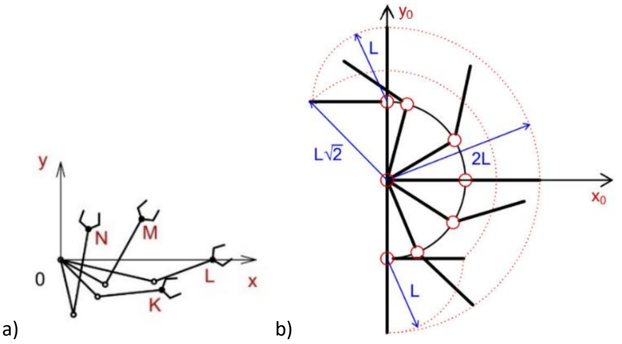

Figure 3. Two-link robotic arm a) in working positions K, L, M, N, b) in various working positions

The next section of the paper describes the procedure for plotting the trajectory of the end point at our selected points. The workspace is also shown. We determined the waveform of angular quantities at the joints of the manipulator and the trajectory of the movement.

4 THE INVERSE KINEMATICS

We have been working on the solution of a two-arm robot with arm lengths L_1 and L_2. The arm is mounted on the fixed base shown in Fig. 4. The rotational kinematic pairs are located at points O_1 and O_2, with the rotation angle θ_1 of the first arm and θ_2 of the second arm. In solving the direct kinematic problem, the kinematic equations (1) and (2) were determined for the positions of the end point M [x_M, y_M] at known angles θ_1 and θ_2:

$$x_M = L_1\cos\theta_1 + L_2\cos(\theta_1 + \theta_2) \quad (1)$$

$$y_M = L_1\sin\theta_1 + L_2\sin(\theta_1 + \theta_2) \quad (2)$$

With the dimensions of the arms of the solved model L_1 =0.4 m and L_2 =0.3 m. We have calculated the masses of the arms m_1=0.4 kg and m_2=0.3 kg. The end point is marked as M. The generalized coordinates describing the above body system are q_1= θ_1 and q_2= θ_2. The coordinate systems of the two arms are shown in Fig. 4. We investigated the motion of the end point M with respect to the reference coordinate system O_0, x_0, y_0, z_0. The member 1 to which the coordinate system O_1, x_1, y_1, z_1 is associated performs a rotational motion with a rotation angle θ_1 about the $z_0 \equiv z_1$ axis, where θ_1= $\theta_1(t)$, with respect to the reference coordinate system. The coordinate system of the second member O_2, x_2, y_2, z_2 is displaced in the x_1 axis direction by a length L_1. Member 2 then performs a rotational motion with a rotation angle θ_2 about the $O_2 \equiv z_2$ axis, where θ_2= $\theta_2(t)$. We have determined the motion of point M on member 2 with length L_2 with respect to the reference coordinate system associated with base 0.

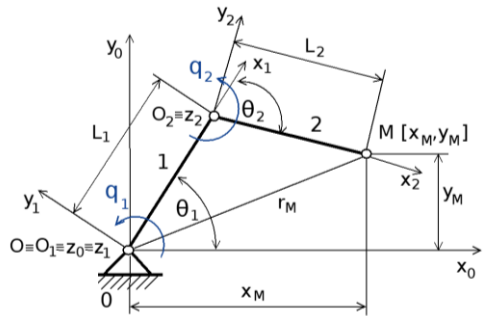

Figure 4. Mechanical system with 2 degrees of freedom and generalized coordinates q_1 and q_2 ($q_1 = \theta_1$ a $q_2 = \theta_2$)

Inverse kinematics refers to the opposite process of direct kinematics. Given the desired location of the end point of the robotic arm x_M, y_M, we needed to determine what the joint rotation angles should be to place the end point of arm M at our desired location. We used equations (1) and (2) again. Here there is usually more than one solution. We can see this in Fig. 5.

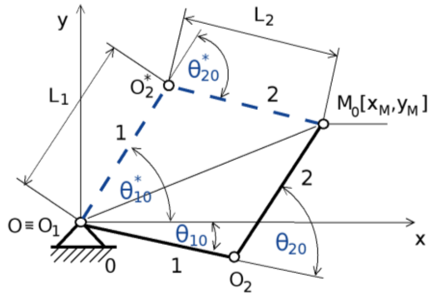

Figure 5. Mechanical system with 2 degrees of freedom and rotation angles θ_{10} a θ_{20} for initial position of the arm and rotation angles θ^*_{10} a θ^*_{20} for final position of the end point

This problem is a typical problem in robotic because we want to achieve a certain position of the end member and for this, we need to determine the angular quantities in the joints to control the movement of the members.

We solved the problem of finding both angles θ_1 and θ_2 from equations (1) and (2). The first angle θ_1 is between the first arm and the base. The second angle θ_2 is between the first arm and the second arm (Fig. 5). Thus, the motion of member 2 and its point M is determined by the angles of rotation θ_1 and θ_2, the angular velocities ω_1 and ω_2, and the angular accelerations α_1 and α_2. We have determined their magnitudes during the motion of the end point M(t=0) from the initial position at time t=0 to the final position of the end point M_1(t=fin) given at time t=t_{fin} according to Fig. 6.

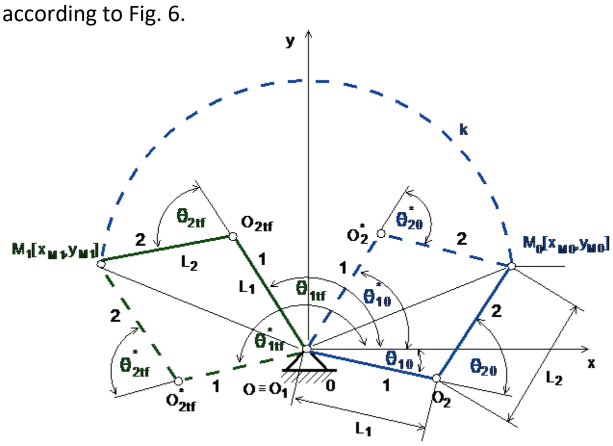

Figure 6. Initial and final position of the point M

We calculated the angles of the arms at the initial position of the M_0 point x_{M0} and y_{M0} and the magnitudes of the angles θ_{10} and θ_{20}. Then we determined the arm angles at the final position of point M_{1tf} x_{M1tf} and y_{M1tf} and the angles θ_{1tf} and θ_{2tf} according to Fig. 6.

We solved the problem while moving the end point of the second arm, between points A, B, C, D and E, whose positions are shown in Tab. 1.

Table 1. Coordinates x_i , y_i of the points A, B, C, D, E

	A	B	C	D	E
x_i [m]	0.3	0.4	0.4	0.3	-0.3
y_i [m]	-0.4	-0.3	0.3	0.4	0.4

By solving the system of equations for the initial and final positions, we determined the corresponding angles of the manipulator arms, which are given in Tab. 2.

Table 2. Respective angles in initial and final points A-B, B-C, C-D, D-E

	A-B	B-C	C-D	D-E
θ_{10}	-90°	0°	0°	90°
	-16.26°	-73.74°	73.74°	16.26°
θ_{20}	90°	-90°	90°	-90°
	-90°	90°	-90°	90°
θ_{1tf}	0°	0°	90°	90°
	-73.74°	73.74°	16.26°	163.74°
θ_{2tf}	-90°	90°	-90°	90°
	90°	-90°	90°	-90°

The values of angles θ_{10}, θ_{20}, θ_{1tf}, θ_{2tf} at the defined points A-B, B-C, C-D, D-E, which we used below to plot the individual trajectories, are shown in Tab. 3.

Table 3. Chosen angles in initial and final points A-B, B-C, C-D, D-E

	A-B	B-C	C-D	D-E
θ_{10}	-90°	-73.74°	73.74°	90°
θ_{20}	90°	90°	-90°	-90°
θ_{1tf}	-73.74°	0°	90°	163.74°
θ_{2tf}	90°	90°	-90°	-90°

The trajectories along which the end point moved between our defined points were determined by solving the direct kinematics.

5 THE FORWARD KINEMATICS

We considered the angle of rotation of arm 1 in the form of a 5th-order polynomial equation:

$$\theta_1(t) = a_1t^5 + a_2t^4 + a_3t^3 + a_4t^2 + a_5t + a_6 \qquad (3)$$

We have considered the angle of rotation of arm 2 in the form:

$$\theta_2(t) = b_1t^5 + b_2t^4 + b_3t^3 + b_4t^2 + b_5t + b_6 \qquad (4)$$

The magnitudes of the initial angles of the arms are known, hence we determined the magnitudes of the coefficients: $a_6 = \theta_1(t=0)$ and $b_6 = \theta_2(t=0)$.

By deriving equations (3) and (4) with respect to time, we obtained the angular velocity, and by further deriving it with respect to time, we obtained the angular acceleration. The magnitude of the angular velocity at the beginning and at the end is zero. The same is true for the angular acceleration. Based on this, we determined the magnitudes of the coefficients: $a_5 = 0$, $a_4 = 0$, $b_5 = 0$, $b_4 = 0$. By solving the system of equations, we calculated the missing coefficients a_3, a_2, a_1, b_3, b_2 and b_1, which are listed in Tab. 4. Considering the position of arm 2 at the defined points, the coefficients b_3, b_2 and b_1 came out to be zero as we expected. This is because the points were determined in such a way that arm 2 relatives to arm 1 did not move.

We then obtained the trajectory for the angular values from Tab. 3, moving the end point through the individual points with the coordinates given in Tab. 1.

Table 4. Coeficients a_i, b_i of the equations (3) and (4), where i=1,2,3

Text	A-B	B-C	C-D	D-E
a_i	0.0532	0.2413	0.0532	0.2413
	-0.2661	-1.2066	-0.2661	-1.2066
	0.3547	1.6088	0.3547	1.6088
b_i	0	0	0	0

The representation of the trajectory $y_i=f(x_i)$ for i=1, 2, 3, 4 of the end point movement from initial position in point A to final position in point B and then from B to C, from C to D and from D to E are shown in Fig. 7.

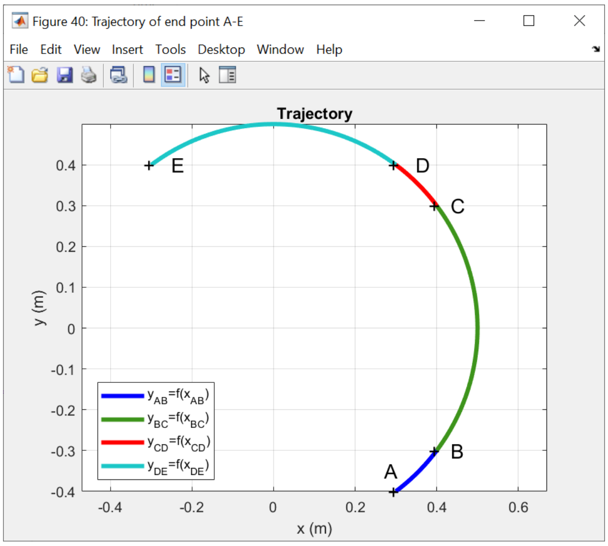

Figure 7. Trajectory components of the end point movement from initial position in point A to position in point B and from point B to point C, C-D and D-E

The trajectory $y_i=f(x_i)$ of the end point movement from the start point A to the point B and then from B to C, C-D and D-E are shown in Fig. 8.

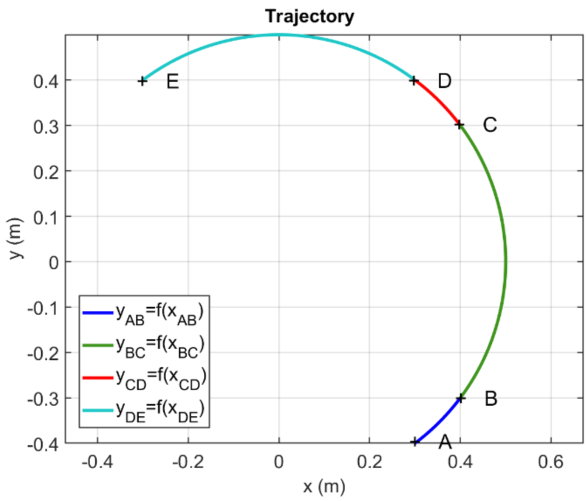

Figure 8. Trajectory components of the end point movement from initial position in point A to position in point B and from point B to point C, C-D and D-E

The solvability of this problem must also be considered in the workspace of the two manipulator arms. The workspace in Fig. 9 is affected by the arm lengths L_1 and L_2 and the working ranges of each joint $q_1 = \theta_1$ a $q_2 = \theta_2$ for angles $-90° \leq \theta_1 \leq 165°$ and angle

-90° ≤ θ_2 ≤ 90°. In Fig. 9, the trajectory of the end point motion between points A-B, B-C, C-D and D-E is shown in the workspace.

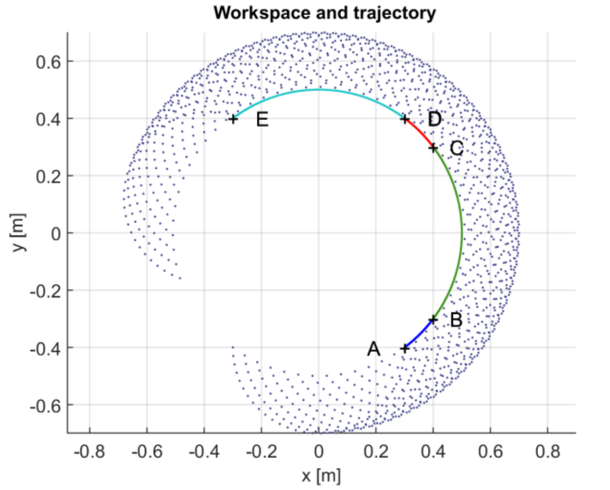

Figure 9. Coordinates x-y for different combinations of θ_1 (-90° ≤ θ_1 ≤ 165°) and θ_2 (-90° ≤ θ_2 ≤ 90°) and trajectory of the end point movement from point A–B, B-C, C-D, D-E

A graphical representation of the kinematic quantities obtained by this method is given in the following sections of the paper.

6 GRAPHIC REPRESENTATION OF KINEMATIC QUANTITIES

In the next step, we determined the angle of rotation θ_1 and θ_2 of arm 1 (Link 1) and arm 2 (Link 2) when moving from the start point A to the end point B, from point B to point C, from point C to point D, and from point D to point E (Fig. 10).

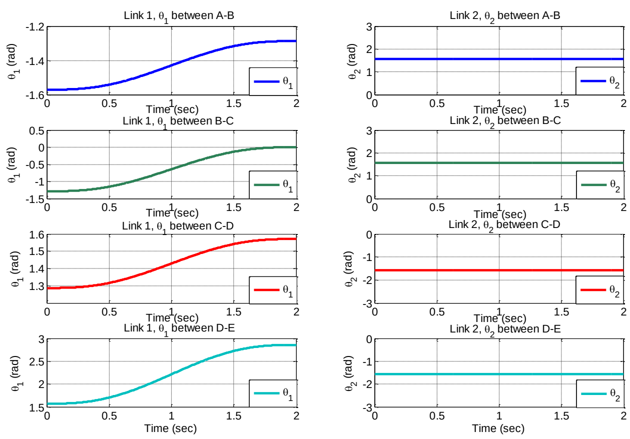

Figure 10. Rotation angles θ_1 and θ_2 of the Link 1 and Link 2 of movement from initial point A to final point B (A-B), B-C, C-D, D-E

The magnitudes of the angle θ_2 of Link 2 when moving in each section are given in degrees in Tab. 3. In Fig. 10, the same angle magnitudes are shown as expected, but they are given in radians. In section A-B, B-C the value is θ_2=1.57 rad and in section C-D, D-E in Fig. 12 the value is θ_2=-1.57 rad, which is the same as in Tab. 3.

Next, the plots of the kinematic parameters of angular velocity and angular acceleration for the movement of the end point of the arms are shown. We have determined the waveform of angular velocity ω_1 and angular acceleration α_1 of arm 1 when moving from the start point A to the end point B, from point B to point C, from point C to point D and from point D to point E in Fig. 11.

The angular velocity ω_2 and angular acceleration α_2 are again zero for each segment, as expected since the angle θ_2 is of constant magnitude.

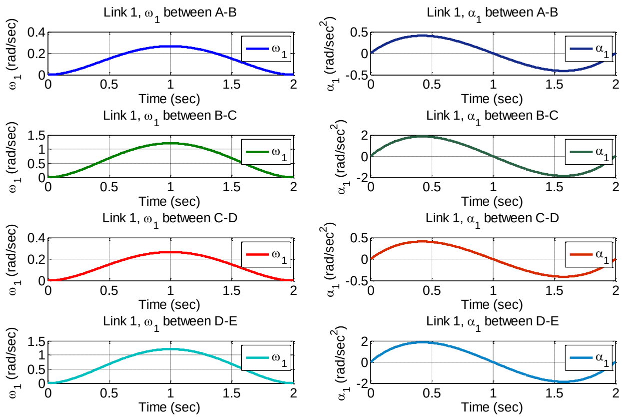

Figure 11. Angular velocity ω_1 and angular acceleration α_1 of the Link 1 (arm 1) of movement from initial point A to final point B (A-B), B-C, C-D, D-E

For the design of the actuators at the individual joints, we are interested in the motion of the arms with the maximum load. Therefore, we have chosen additional points A_1, E_1 and E_2. The position of points A_1, E_1 and E_2 was chosen to investigate the motion of the arms with maximum load. The position of each point is shown in Tab. 5.

Table 5. Coordinates x_i , y_i of the points A_1, E_1, E_2

	A_1	E_1	E_2
x_i [m]	0.0	-0.7	-0.1
y_i [m]	-0.7	0.0	0.0

The values of angles θ_{10}, θ_{20}, θ_{1tf}, θ_{2tf} at the defined points A-A_1, A_1-E_1, E_1-E_2, which we used below to plot the individual trajectories, are shown in Tab. 6.

Table 6. Respective angles in initial and final points A-A_1, A_1-E_1, E_1-E_2

	A-A_1	A_1-E_1	E_1-E_2
θ_{10}	-90°	-90°	180°
θ_{20}	90°	0°	0°
θ_{1tf}	-90°	180°	180°
θ_{2tf}	0°	0°	180°

The plots of the position y=f(x) of the end point movement from point A to A_1 and further A_1-E_1, E_1-E_2 are shown in Fig. 12.

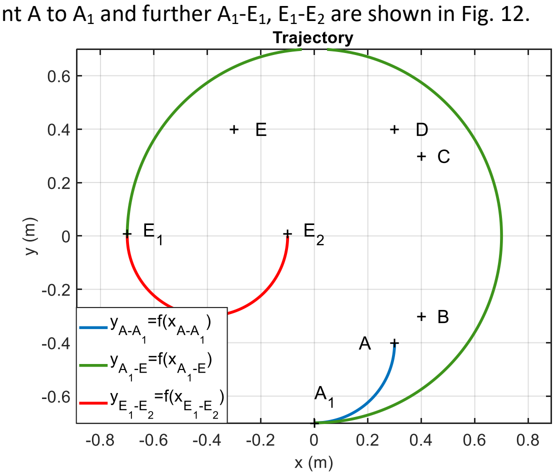

Figure 12. Trajectory of the end point movement from point A–A_1, A_1-E_1, E_1–E_2

Coefficients a_1, a_2, a_3, b_1, b_2, b_3 of movement from initial point A to final point A_1, from point A_1 to point E_1 and from point E_1 to E_2 are in Tab. 7. The positions of the end points at different combinations of the angles θ_1 and θ_2 are shown in the next Fig.

Table 7. Coeficients a_i , b_i

Text	A- A_1	A_1- E_1	E_1- E_2
a_i	0	0.8836	0
	0	-4.4179	0
	0	5.8905	0
b_i	-0.2945	0	0.5890
	1.4726	0	-2.9452
	-1.9635	0	3.9270

The position of the end point and workspace for angle constraints -90° ≤ θ_1 ≤ 180° and -175° ≤ θ_2 ≤ 175° during the motion of the manipulator from point A to A_1, A_1 to E_1, and from E_1 to E_2 with arms with lengths L_1=0.4 m and L_2=0.3 m are shown in Fig. 13.

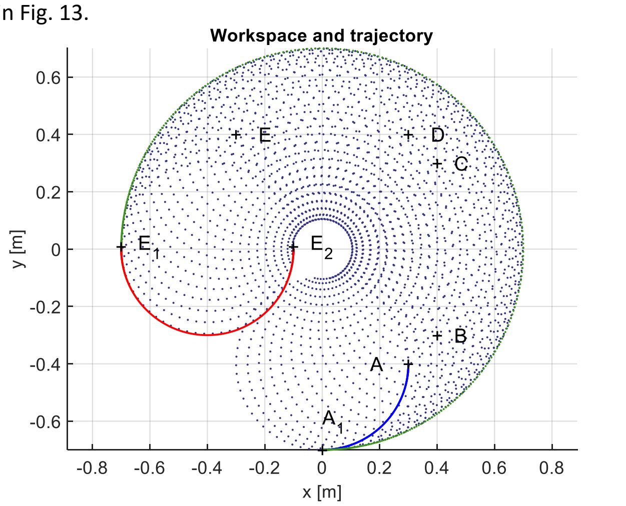

Figure 13. Coordinates x-y for different combinations of angles θ_1 and θ_2 for angle constraint -90° ≤ θ_1 ≤ 180°, angle constraint -175° ≤ θ_2 ≤ 175° and trajectory from point A–A_1, A_1-E_1, E_1–E_2

The rotation angle θ_1 and θ_2 with known trajectory of the end point is shown in Fig. 14.

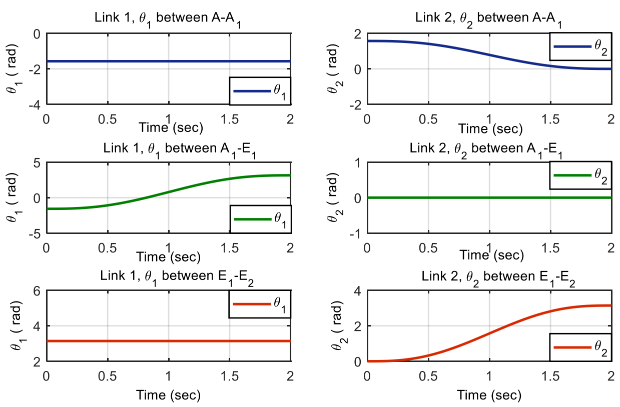

Figure 14. Rotation angle θ_1 and θ_2 of the end point movement from point A–A_1, A_1-E_1, E_1–E_2

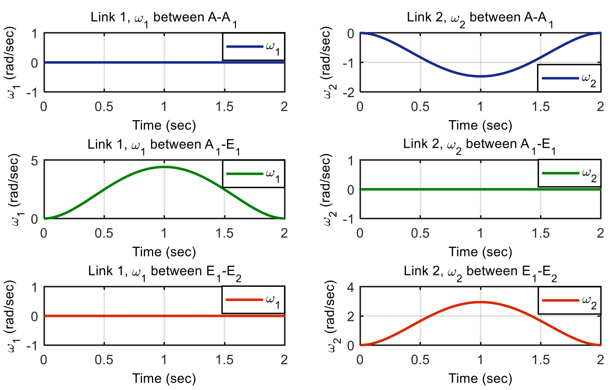

Figure 15. Angular velocities ω_1 and ω_2 of the end point movement from point A–A_1, A_1-E_1, E_1–E_2

The angular velocity of arms with lengths L_1=0.4 m and L_2=0.3 m is shown in Fig. 15.

The angular acceleration of arms with lengths L_1=0.4 m and L_2=0.3 m is shown in Fig. 16.

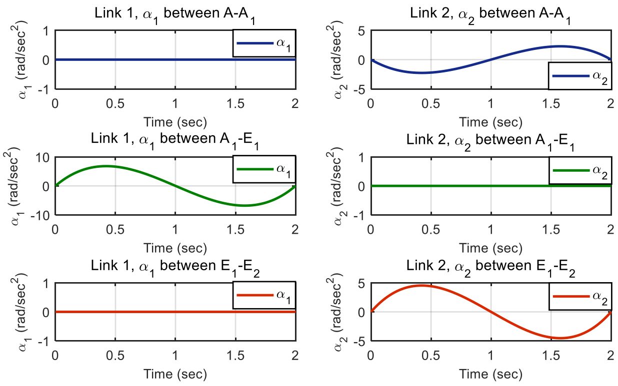

Figure 16. Angular accelerations α_1 and α_2 of the end point movement from point A–A_1, A_1-E_1, E_1–E_2

The determined angular quantities shown in Figs. 14-16 were subsequently used to solve the inverse dynamics problem and determine the magnitude of the torques at the individual joints.

7 INVERSE AND FORWARD DYNAMICS

Our goal in this section was to determine the magnitude of the torque or driving forces and the motion generators for the desired motion of the robot end point. The analyzed manipulator model (Fig. 4) was simulated in the Matlab add-on program - SimMechanics.

Fig. 17 shows the applied action driving moments τ_1 and τ_2, which were determined using the inverse dynamics problem.

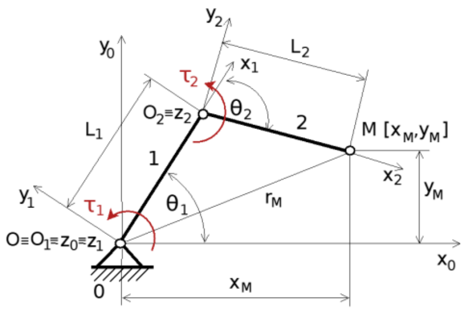

Figure 17. Two-link robotic arm with joint torques τ_1 and τ_2

The equations of motion (5) of the dynamic system are written:

$$M(\theta)\ddot{\theta} + V(\theta,\dot{\theta}) + G(\theta) = \tau \qquad (5)$$

where

τ – the vector of actuator torques, $M(\theta)$ – the inertia matrix, $V(\theta,\dot{\theta})$ – the Coriolis centripetal vector and $G(\theta)$ = – the gravity vector.

Equation (5) in our case of two-link manipulator represents a system of two 2nd order differential equations.

The block diagram in SimMechanics for calculation of these torques is in Fig. 18.

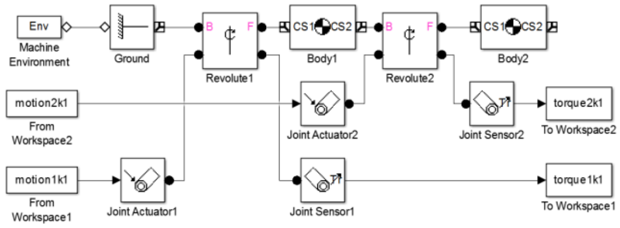

Figure 18. SimMechanics block diagram for determining torques τ_1 and τ_2 in joint of member 1 (Link 1) and member 2 (Link 2)

Verification of the accuracy of the calculation is possible by substituting the obtained results into the forward dynamics problem. The respective block diagram in SimMechanics is shown in Fig. 19.

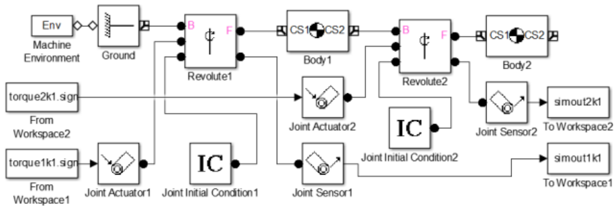

Figure 19. SimMechanics block diagram for determining the angular motion produced by torques τ_1 and τ_2 in joints of member 1 and member 2

The blocks IC (Initial Conditions) in Fig. 19 define the values of the angles θ_{10} a θ_{20} at the beginning of the motion.

Results graphs of the joint torques τ_1 a τ_2 are shown in Figs. 20 to 23. Using SimMechanics in the Matlab/Simulink with the inverse dynamic problem we obtained driving torques τ_1 a τ_2 in Tab. 8 in respective joints of the manipulator for end point that moves from start point A to end point B, from start point B to end point C, C-D and D-E. Mass of the arm m_1=0.4 kg, m_2=0.3 kg. Maximum torque magnitudes are τ_1 = 2.5178 Nm and τ_2 = 0.4832 Nm (Fig. 20).

Table 8. Torques τ_1 and τ_2 in the joint when end point moves from A-B, B-C, C-D, D-E

	A-B	B-C	C-D	D-E
τ_1	2.4643	2.5178	2.4645	2.5174
τ_2	0.4573	0.4832	0.4573	0.4832

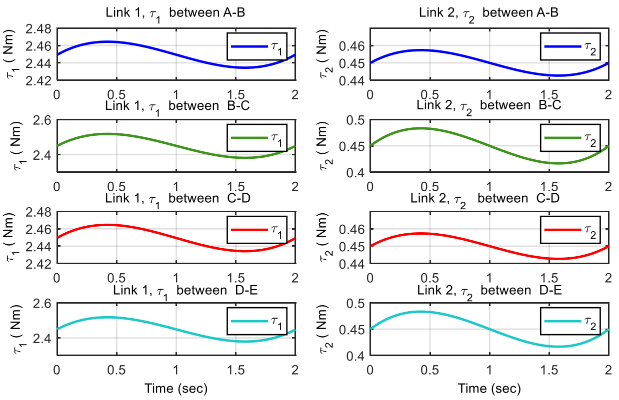

Figure 20. Torques τ_1 and τ_2 of the joint, where m_1=0.4 kg, m_2=0.3 kg

Resulting torques τ_1 and τ_2 of the mass of the arm m_1=0.4 kg, m_2=0.3 kg for end point that moves from A-A_1, A_1-E_1, E_1-E_2 are shown in Tab. 9 and Fig. 21. Maximum torque magnitudes are τ_1 = 2.6992 Nm and τ_2 = 0.5714 Nm.

Table 9. Torques τ_1 and τ_2 in the joint when the end point moves from A–A_1, A_1-E_1, E_1–E_2, m1=0.4 kg, m2=0.3 kg

	A-A_1	A_1-E_1	E_1-E_2
τ_1	2.4896	2.6992	2.5272
τ_2	0.4896	0.5714	0.5288

Resulting torques τ_1 and τ_2 of the mass of the arm m_1=0.4 kg, m_2=0.8 kg for end point that moves from A-A_1, A_1-E_1, E_1-E_2 are shown in Tab. 10 and Fig. 22. Maximum torque magnitudes are τ_1 = 5.4665 Nm and τ_2 = 1.3261 Nm.

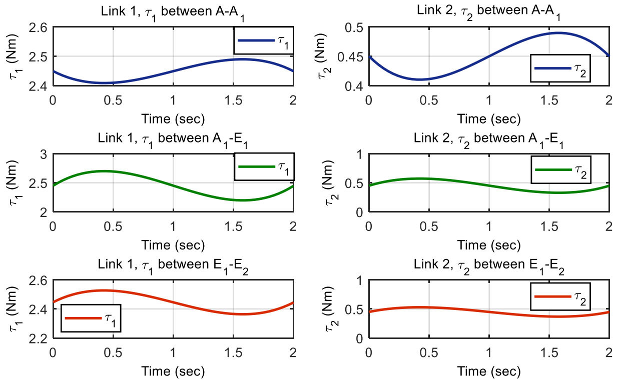

Figure 21. Torques τ_1 and τ_2 of the joint, where m_1=0.4kg, m_2=0.3kg

Table 10. Torques τ_1 and τ_2 in the joint when end point moves from A–A_1, A_1-E_1, E_1–E_2, where m_1=0.4kg, m_2=0.8kg

	A-A_1	A_1-E_1	E_1-E_2
τ_1	5.2402	5.4665	5.2762
τ_2	1.2398	1.3261	1.2784

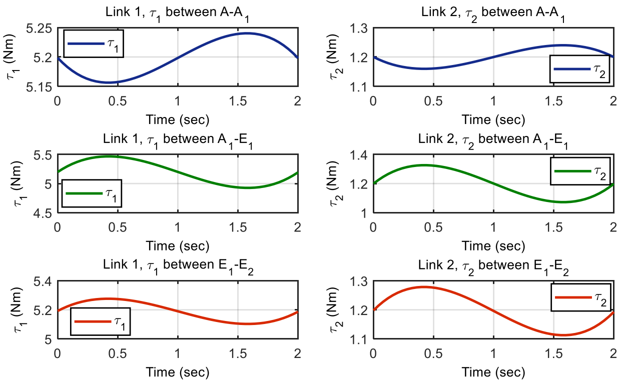

Figure 22. The torques τ_1, τ_2 in joint, m_1=0.4 kg, m_2=0.8 kg

Resulting torques τ_1 and τ_2 of the mass of the arm m_1=0.4 kg, m_2=1.3 kg for end point that moves from A-A_1, A_1-E_1, E_1-E_2 are shown in Tab. 11 and Fig. 23. Maximum torque magnitudes are τ_1 = 8.2338 Nm and τ_2 = 2.0808 Nm.

Table 11. Torque τ_1 and τ_2 of the joint when the end point moves from A–A_1, A_1-E_1, E_1–E_2, m1=0.4 kg, m2=1.3 kg

	A-A_1	A_1-E_1	E_1-E_2
τ_1	7.9909	8.2338	8.0251
τ_2	1.9900	2.0808	2.0280

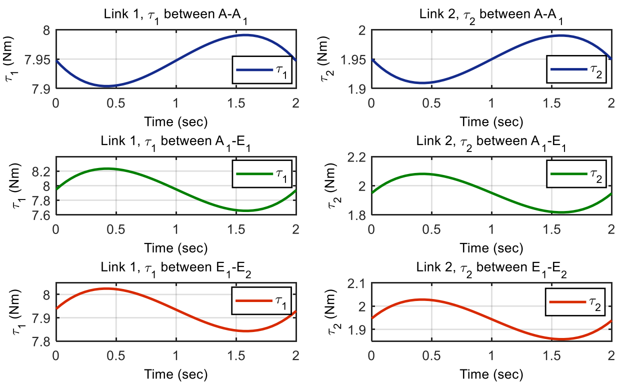

Figure 23. The torques τ_1, τ_2 in joint, m_1=0.4 kg, m_2=1.3 kg

The above methodology was used to determine the magnitudes of the moments in the joints of both arms. Different trajectories for the movement of the end point of the arms were chosen. As expected, the maximum values of the magnitudes of the moments were obtained in the sections of motion with the maximum unloading of the arms. As expected, the magnitude of the moments also increased by increasing the load on the second member.

CONCLUSIONS

In this paper, a procedure for solving the kinematics and dynamics analysis of a two-link open kinematic chain robot was presented. The solution was implemented in Matlab.

The paper dealt with inverse and direct kinematic problems. As a result, the waveform of the rotation angle of both arms of the model was obtained. Furthermore, the trajectory of the manipulator end point was determined as it moved through the defined points. Subsequently, the trajectories of the rotation angle, angular velocity and angular acceleration of the two arms were determined in the form of graphs.

By solving the inverse dynamics problem, the waveforms of the moments in the kinematic pairs of arms 1 and arm 2 were determined. The torques waveforms required to perform the desired motion along the trajectory determined by the start and end point were determined.

Matlab computer simulation capabilities were implemented on a fixed base manipulator model. The simulation gives instantaneous information about the magnitudes of the parameters of the model being solved. The computer simulation allows rapid change of the model parameters. Matlab program is advantageously used to simulate the motion of mechanical systems of industrial robots and manipulators. This presented methodology provides a suitable tool for solving problems of teaching but also for the needs of practice.

ACKNOWLEDGMENTS

The authors would like to thank to Slovak Grant Agency projects VEGA 1/0201/21 and VEGA 1/0436/22, grant project KEGA 031 TUKE-4/2022 and grant project KEGA 027 TUKE-4/2022 supported by the Ministry of education of Slovak Republic.

REFERENCES

[Bozek 2014] Bozek, P., Turygin, Y. Measurement of the operating parameters and numerical analysis of the mechanical subsystem. Measurement Science Review, 2014, Vol. 14, No. 4, pp. 198-203.

[Bozek 2021] Bozek, P., Nikitin, Y., Krenicky, T. The Basics Characteristics of Elements Reliability. In: Diagnostics of Mechatronic Systems. Series: Studies in Systems, Decision and Control, 2021, Vol. 345, pp. 1-15. ISBN 978-3-030-67055-9.

[Carbone 2016] Carbone G., Di Nuovo A. A hybrid multi-objective approach for optimal path planning of a hexapod robot a preliminary study. Lecture Notes in Computer Science, 2016, Vol. 9668, pp. 131-144.

[Delyova 2014] Delyova, I., et al. Kinematic analysis of crank rocker mechanism using MSC Adams/View. Applied Mechanics and Materials, 2014, pp. 90-97.

[Dyadyura 2021] Dyadyura, K., Hrebenyk, L., Krenicky, T., Zaborowski, T. Modeling of the Manufacturing Systems State in the Conditions of the Lean Production. MM Science Journal, 2021, Vol. June, pp. 4408-4413.

[Frankovsky 2013] Frankovsky, P., et al. Modeling of Dynamic Systems in Simulation Environment MATLAB/Simulink SimMechanics. American Journal of Mechanical Engineering, 2013, Vol. 1, No. 7, pp. 282-288.

[Garcia 2015] Garcia, F. J. A. et al. Simulators based on physical modeling tools to support the teaching of automatic control (2): rotating pendulum. In: Proc. of the 36th Conf. on Automation, 2015, Bilbao, pp. 667-673.

[Hargas 2015] Hargas, L.A. et al. Regular Shapes Detection for Analysis of Biomedical Image Sequences. In: Int. Conf. on Applied Electronics (AE). Pilsen, Sep 08-09, 2015, pp. 49-52.

[Holubek 2014] Holubek, R., Ruzarovsky, R. The methods for increasing of the efficiency in the intelligent assembly cell. Applied Mechanics and Materials, 2014, Vol. 470, pp. 729-732. doi:10.4028/www.scientific.net/AMM.470.729.

[Hroncova 2012] Hroncova, D., Binda, M., Sarga, P., Kicak, F. Kinematical analysis of crank slider mechanism using MSC Adams/View. Procedia Engineering, 2012, Vol. 48, pp. 213-222.

[Hroncova 2012] Hroncova, D., Sarga, P., Gmiterko, A. Simulation of mechanical system with two degrees of freedom with Bond Graphs and Matlab/Simulink. Procedia Engineering, 2012, Vol. 48, pp. 223-232.

[Hroncova 2019] Hroncova, D., et al. Simulation in Matlab/Simulink. Kosice, TU Kosice, 2019. ISBN 978-80-553-3470-7.

[Hroncova 2022a] Hroncova D., et al. Forward and inverse robot model kinematics and trajectory planning, In: Mechatronika 2022: 20th Int. Conf. on Mechatronics, Pilsen, Czech Republic. Danvers (USA), 2022, pp. 348-356. ISBN 978-1-6654-1048-9.

[Hroncova 2022b] Hroncova, D. et al. Robot Trajectory Planning. MM Science Journal, 2022, Vol. November, pp. 6098-6108. doi: 10.17973/MMSJ.2022_11_2022093.

[Hunady 2019] Hunady, R., et al. Modeling of mechanical systems in the MSC Adams. Kosice, TU Kosice, 2019. ISBN 978-80-553-3471-4.

[Kelemen 2014] Kelemen, M., et al. Rapid Control Prototyping of Embedded Systems Based on Microcontroller. Procedia Engineering, 2014, Vol. 96, Issue 11, pp. 215-220. ISSN 1877-7058.

[Kelemen 2021] Kelemen, M. et al. Head on Hall Effect Sensor Arrangement for Displacement Measurement. MM Science Journal, 2021, Vol. October, pp. 4757-4763.

[Kelemenova 2021] Kelemenova, T., et al. Verification of Force Transducer for Direct and Indirect Measurements. MM Science Journal, 2021, Vol. October, pp. 4736-4742.

[Kurylo 2018] Kurylo, P. Experimental Stand for Actuator Testing. Acta Mechatr., 2018, Vol. 3, No. 2, pp. 7-10.

[Lestach 2022] Lestach, L., et al. Two-legged Robot Concepts. MM Science Journal, 2022, Vol. October, pp. 5812-5818. ISSN 1803-1269.

[Mikova 2014] Mikova, L., et al. Simulation Model of Manipulator for Model Based Design. Applied Mechanics and Materials, 2014, Vol. 611, No. 1, pp. 175-182.

[Mikova 2016] Mikova, L., et al. Impact of dynamics of the frame on the performance of the positioning servosystem. Int. J. of Adv. Robotic Systems, 2016, Vol. 13, No. 5, pp. 1-6.

[Mikova 2022] Mikova, L. et al. Upgrade of Biaxial Mechatronic Testing Machine for Cruciform Specimens and Verification by FEM Analysis. Machines, 2022, Vol. 10, No. 10. doi.org/10.3390/machines10100916.

[Nikitin 2020] Nikitin, Y., Bozek, P., Peterka, J. Logical-Linguistic Model of Diagnostics of Electric Drives with Sensors Support. Sensors, 2020, Vol. 20, No. 16.

[Nikitin 2022] Nikitin, Y. R., Krenický, T., Bozek, P. Diagnostics of automated technological drives. Lüdenscheid: RAM-Verlag, 2022, 148 p. <https://ram-verlag.org/vol-6-diagnostics-of-automated-technological-drives>.

[Papacz 2018] Papacz, W. Didactic models of manipulators. Acta Mechatronica, 2018, Vol. 3, No. 3, pp. 7-11.

[Peterka 2020] Peterka, J., Nikitin, Y., Bozek, P. Diagnostics of automated technological devices. MM Science Journal, 2020, Vol. October, pp. 4027-4034.

[Pirnik 2016] Pirnik, R., Hrubos, M., Nemec, D., Bozek, P. Navigation of the autonomous ground vehicle utilizing low-cost inertial navigation. Acta Mechatronica, 2016, Vol. 1, No. 1, pp. 19-23.

[Pivarciova 2022] Pivarciova, E. et al. Use of Holographic Interferometry for Monitoring Heat Transfer. MM Science Journal, 2022, Vol. March, pp. 5522-5525.

[Ruzarovsky 2019] Ruzarovsky, R., et al. A case study of robotic simulations using virtual commissioning supported by the use of virtual reality. In: 14th Int. Conf. on Modern Technologies in Manufacturing (MTeM), 2019, Vol. 299, Art. No. 02006. doi: 10.1051/matecconf/201929902006.

[Saga 2018] Saga, M., et al. Effective algorithm for structural optimization subjected to fatigue damage and random excitation. Scientific Journal of Silesian University of Technology-Series Transport, 2018, Vol. 99, doi: 10.20858/sjsutst.2018.99.14.

[Saga 2020] Saga, M., et al. Case study: Performance analysis and development of robotized screwing application with integrated vision sensing system for automotive industry. Int. J. of Adv. Robotic Systems, 2020, Vol. 17, No. 3.

[Sapietova 2018] Sapietova, A., et al. Application of optimization algorithms for robot systems designing. Int. J. of Adv. Robotic Systems, 2018, Vol. 15, No. 1, pp. 1-10.

[Semjon 2016] Semjon, J., et al. Testing of parameters of proposed robotic wrist based on the precision modules. Int. J. of Adv. Robotic Systems, 2016, Vol. 13, pp. 1-7. ISSN 1729-8814.

[Semjon 2020] Semjon, J., et al. Verification of the UR5 robot's properties after a crash caused by a fall of a transferred load from a crane. Int. J. of Adv. Robotic Systems, 2016, Vol. 17, pp. 1-9. ISSN 1729-8814.

[Serrano 2015] Serrano, J. et al. Simulators Based on Physical Modeling Tools to Support the Teaching of Automatic Control (I): Mobile Robot with Flexible Arm. In: 36th Conf. on Automation. Bilbao: Minutes Book, 2015, pp. 659-666.

[Simonova 2017] Simonova, A., et al. Uses of on–off controller for regulation of higher-order system in comparator mode. Electr. Eng., 2017, Vol. 99, pp. 1367-1375. https://doi.org/10.1007/s00202-017-0610-7.

[Sincak 2021] Sincak, P.J., et al. Chimney Sweeping Robot Based on a Pneumatic Actuator. Applied Sciences, 2021, Vol. 11, No. 11, 4872. https://doi.org/10.3390/app11114872.

[Smrcek 2003] Smrcek, J., Palko, A., Nemec, M. Some problems in design of wheeled mobile robot undercarriadge. Acta Mech. Slovaca, 2003, Vol. 7, Iss. 3, pp. 129-136.

[Tedeschi 2015] Tedeschi, F., Carbone, G. Hexapod Walking Robot Locomotion. Mechanisms and Machine Science, 2015, Vol. 29, pp. 439-468.

[Tedeschi 2017] Tedeschi, F., Carbone, G. Design of a novel leg-wheel hexapod walking robot. Robotics, 2017, Vol. 6, No. 4.

[Tlach 2019] Tlach, V., Kuric, I., Sagova, Z., Zajacko, I. Collaborative assembly task realization using selected type of human-robot interaction. Transportation Research Procedia, 2019, Vol. 40. doi: 10.1016/j.trpro.2019.07.078, 2019.

[Trojanova 2021] Trojanova, M., Cakurda, T., Hosovsky, A., Krenicky, T. Estimation of Grey-Box Dynamic Model of 2-DOF Pneumatic Actuator Robotic Arm Using Gravity Tests. Applied Sciences, 2021, Vol. 11, No. 10, Art. No. 4490.

[Vagas 2011] Vagas, M., et al. The view to the current state of robotics. International Proceedings of Computer Science and Information Technology, 2011, Vol. 8, pp. 205-209.

[Vagas 2022] Vagas, M., et al. Testing of Ethernet-based communication between control PLC and collaborative mechatronic system. In: 20th Int. Conf. on Mechatronics. 10.1109/ME54704.2022.9983428.

[Vagas 2023] Vagas, M., et al. Calibration of an intuitive machine vision system based on an external high-performance image processing unit. In: 24th Int. Conf. on Process Control. 2023, pp. 186-191. doi: 10.1109/PC58330.2023.10217606

[Virgala 2012] Virgala, I., et al. Manipulator End-Effector Position Control. Procedia Engineering, 2012, Vol. 48, pp. 684-692. ISSN 1877-7058.

[Virgala 2014] Virgala, I., et al. Analysing, Modeling and Simulation of Humanoid Robot Hand Motion. Procedia Engineering, 2014, Vol. 611, pp. 75-82.

[Virgala 2020] Virgala, I. et al. Reconfigurable Wheel-Legged Robot. MM Science Journal, 2020, Vol. June, pp. 3960-3965.

[Virgala 2022] Virgala, I., et al. A Non-Anthropomorphic Bipedal Walking Robot with a Vertically Stabilized Base. Appl. Sciences, 2022, Vol. 12, 4108.

[Volak 2019] Volak, J., et al. Interference artifacts suppression in systems with multiple depth cameras. In: 42nd Int. Conf. on Telecommunications and Signal Processing. Budapest, Jul 01-03, 2019, pp. 472-476. doi: 10.1109/TSP.2019.8768877.

[Zidek 2018] Zidek, K., et al. Auxiliary Device for Accurate Measurement by the Smart vision System. MM Science Journal, 2018, Vol. March, pp. 2136-2139.

[Zivcak 2023] Zivcak, J., Material development in personalized implantology, 1st Ed. Kosice: TUKE, 2023, 178 p. ISBN 978-80-553-4415-7.

CONTACTS:

doc. Ing. Patrik Sarga, Ing., PhD.
Technical University of Kosice, Faculty of Mechanical Engineering
Institute of Automation, Mechatronics, Robotics and Production Techniques
Letna 9, 04200 Kosice, Slovak Republic
patrik.sarga@tuke.sk